Published in final edited form as:
Eur J Neurosci. 2006 May ; 23(10): 2635–2647.

Clearance and prevention of prion infection in cell culture by anti-PrP antibodies

Joanna Pankiewicz[1,*], **Frances Prelli**[1,*], **Man-Sun Sy**[5], **Richard J. Kascsak**[4], **Regina B. Kascsak**[4], **Daryl S. Spinner**[4], **Richard I. Carp**[4], **Harry C. Meeker**[4], **Marcin Sadowski**[1,2], and **Thomas Wisniewski**[1,2,3,4]

1 *Department of Neurology, New York University School of Medicine, 550 First Avenue, New York NY 10016, USA*

2 *Department of Psychiatry, New York University School of Medicine, 550 First Avenue, New York NY 10016, USA*

3 *Department of Pathology, New York University School of Medicine, 550 First Avenue, New York NY 10016, USA*

4 *New York State Institute for Basic Research in Developmental Disabilities, 1050 Forest Hill Road, Staten Island, NY 10314, USA*

5 *Departments of Pathology and Neuroscience, Case Western Reserve University School of Medicine, 10900 Euclid Ave., Cleveland, OH 44106, USA*

Abstract

Prion diseases are transmissible and invariably fatal neurodegenerative disorders associated with a conformational transformation of the cellular prion protein (PrP^{C}) into a self-replicating and proteinase K (PK)-resistant conformer, scrapie PrP (PrP^{Sc}). Humoral immunity may significantly prolong the incubation period and even prevent disease in murine models of prionoses. However, the mechanism(s) of action of anti-PrP monoclonal antibodies (Mabs) remain(s) obscure. The murine neuroblastoma N2a cell line, infected with the 22L mouse-adapted scrapie strain, was used to screen a large library of Mabs with similar binding affinities to PrP, to identify those antibodies which could clear established infection and/or prevent infection de novo. Three Mabs were found capable of complete and persistent clearing of already-infected N2a cells of PrP^{Sc}. These antibodies were 6D11 (generated to PK-resistant PrP^{Sc} and detecting PrP residues 93–109), and 7H6 and 7A12, which were raised against recombinant PrP and react with neighbouring epitopes of PrP residues 130–140 and 143–155, respectively. Mabs were found to interact with PrP^{Sc} formation both on the cell surface and after internalization in the cytosol. Treatment with Mabs was not associated with toxicity nor did it result in decreased expression of PrP^{C}. Both preincubation of N2a cells with Mabs prior to exposure to 22L inoculum and preincubation of the inoculum with Mabs prior to infecting N2a cells resulted in a significant reduction in PrP^{Sc} levels. Information provided in these studies is important for the rational design of humoral immune therapy for prion infection in animals and eventually in humans.

Keywords

conformational disorder; monoclonal antibodies; N2a cell line; scrapie; treatment

Correspondence: Dr Thomas Wisniewski, MHL Rm HN419, or Dr Marcin Sadowski, RR Rm 207, New York University School of Medicine, 550 First Avenue, New York NY 10016, USA. E-mail: Thomas.Wisniewski@med.nyu.edu or Marcin.Sadowski@med.nyu.edu.

*J.P. and F.P. contributed equally to this study.

Abbreviations

ATCC, American Type Culture Collection; BSE, bovine spongiform encephalopathy; Mab, monoclonal antibody; MEM, minimal essential medium; MTT, 3-(4,5-dimethylthiazol-2-yl)2,5-diphenyltetrazolium bromide; N2a/22L cells, N2a cells infected with the 22L mouse-adapted scrapie strain; PK, proteinase K; PrP^{C}, cellular prion protein; PrP^{Sc}, scrapie prion protein; recPrP, recombinant PrP; vCJD, variant Creutzfeldt – Jakob disease

Introduction

Currently no effective treatment for prion diseases exists. As a result of the bovine spongiform encephalopathy (BSE) epidemic large populations have been exposed to this animal prion disease with the potential for human transmission. In the United Kingdom alone, the total number of definite or probable cases of variant Creutzfeldt–Jakob disease (vCJD) has currently reached 160 patients, who contracted the infection from prion-contaminated beef products (UK Department of Health & Monthly CJD Statistics, 2006). Due to the very long incubation period of prionoses, it has been suggested that a much larger number of people could be asymptomatic carriers of this disease (Balter, 2002; Hilton *et al*., 2002). This cohort is at risk of developing disease in the future and also constitutes a reservoir of infectivity. Transmissibility of prions through blood products has been experimentally shown with the induction of scrapie in sheep by blood transfusion from BSE cattle (Houston *et al*., 2000). Furthermore, scrapie prion protein (PrP^{Sc}) was detected in the lymphatic system of a patient who had received blood products donated by an asymptomatic prion carrier (Peden *et al*., 2004). Spread of infection from asymptomatic carriers is possible because of the accumulation of PrP^{Sc} in the lymphatic system long before the appearance of clinical disease (Wadsworth *et al*., 2001; Hilton *et al*., 2004a,b). The presence of PrP^{Sc} may remain limited to the extraneural tissues for a prolonged period (Eklund *et al*., 1967; Rubenstein *et al*., 1991; Yasuhara *et al*., 1993; Herzog *et al*., 2004); therefore, PrP^{Sc} formation can be targeted in the early stages of infection by treatment approaches which do not have to be capable of penetrating the blood–brain barrier.

Reports from several laboratories have demonstrated that immunization can significantly prolong the incubation period of prionoses or even prevent disease symptoms (Goni *et al*., 2005; Sigurdsson *et al*., 2002a; Schwarz *et al*., 2003). The effectiveness of these approaches appears to be associated chiefly with humoral immunity (Heppner *et al*., 2001; Sigurdsson *et al*., 2003; White *et al*., 2003). However, the exact mechanism by which anti-PrP antibodies interfere with PrP^{Sc} formation remains obscure. Analysis of *in vitro* and *in vivo* treatment studies indicated that only some anti-PrP monoclonal antibodies (Mabs) demonstrate therapeutic efficacy (Peretz *et al*., 2001; Sigurdsson *et al*., 2003; Perrier *et al*., 2004; Feraudet *et al*., 2005). Therefore, understanding how Mabs interfere with PrP^{Sc} formation, and selecting those Mabs which are therapeutically active, is crucial for the rational design of the humoral immune therapy for prion infection. Hypotheses for the mechanisms of action of Mabs include perturbation of PrP^{C} trafficking by Mabs (Feraudet *et al*., 2005), lowering PrP^{C} content (Perrier *et al*., 2004), interference with the interaction of PrP^{C} and PrP^{Sc} (Peretz *et al*., 2001) and sequestration of PrP^{C} and/or PrP^{Sc} on the cell surface by Mabs (Enari *et al*., 2001a; Kim *et al*., 2004). In this study we used N2a murine neuroblastoma cell lines susceptible to infection with the 22L mouse-adapted scrapie strain (Bosque & Prusiner, 2000; Nishida *et al*., 2000; Perrier *et al*., 2004) to test the effectiveness of a number of Mabs for their ability both to prevent and to clear established infection. We attempted to map PrP^{Sc} epitopes which are the most crucial for the propagation of prion infectivity.

Materials and methods

Cell lines were purchased from American Type Culture Collection (ATCC; Manassas, VA, USA). Animals were obtained from Taconic (Germantown, NY, USA). All reagents and antibodies used in this study were purchased from Sigma (St Louis, MO, USA) unless specified otherwise. Animal studies were approved by the NYU School of Medicine Institutional Animal Care and Use Committee and were consistent with the recommendations of the American Veterinary Association.

Infection of N2a cells with 22L mouse-adapted prion strain

N2a mouse neuroblastoma cells (ATCC line CCL 131) were maintained in minimal essential medium (MEM) supplemented with heat-inactivated 10% fetal bovine serum, penicillin (100 units/mL) and streptomycin (100 μg/mL) at 37 °C in 5% CO_2. Brains of terminally sick CD-1 mice infected with mouse-adapted 22L prion strain were homogenized by sonication (10% weight/volume) in cold phosphate-buffered saline and 5% dextrose in sterile conditions. For infection the brain homogenate was further diluted to 2% in Opti-MEM and added to subconfluent six-well plates (Corning, Acton, MA, USA), 1 mL per 10-cm^2 well. After 5 h, 1 mL of regular MEM was added and the cells were incubated in the presence of infectious brain homogenate for an additional 12 h. After the medium was replaced with standard MEM, N2a cells were grown until confluence and then they were split into 1 : 2 dilutions and transferred to 25-cm^2 flasks (Corning). Cells grown in one of the flasks were split 1 : 2 every 4–5 days to give rise to subsequent passages, whereas cells grown in the other flask were harvested and homogenized to monitor the level of PrP^{Sc} (see below). As a control experiment N2a cells were exposed to other mouse-adapted scrapie strains including 87V, 139A and ME7 in experimental conditions analogous to these described above. Previously published data indicate that wild-type N2a cells are resistant to infection with these strains (Bosque & Prusiner, 2000; Nishida *et al*., 2000).

Detection and quantification of PrP^{Sc} in infected N2a cells (N2a/22L)

N2a cells infected with the 22L mouse-adapted scrapie strain (N2a/22L) were harvested using ice-cold lysis buffer [NaCl, 150 mM; triton X-100, 0.5%; sodium deoxycholate, 0.5%; and Tris-HCL, 50 mM, pH 7.5; with a protease inhibitor cocktail (Roche, Indianapolis, IN, USA)]. The lysates were centrifuged for 3 min at 10 000 ***g*** to remove cell debris and the total protein concentration was measured in the supernatant using the bicinchoninic acid assay (BCA; Pierce, Rockford, IL, USA). Aliquots containing 200 μg of total protein were titrated by adding buffer to achieve a final protein concentration of 1 μg/μL. Samples were digested with proteinase K (PK; Roche) for 30 min at 37 °C. The enzyme-to-protein weight ratio was 1 : 50 (Perrier *et al*., 2004). PK activity was quenched by adding phenylmethanesulphonyl fluoride to achieve a final concentration of 3 mM. Samples were then centrifuged at 20 000 ***g*** for 45 min at 4° C. Pellets were resuspended in 15 μL Tris-buffered saline and 15 μL sample buffer, boiled for 5 min and then subjected to electrophoresis on 12.5% SDS-polyacrylamide Tris-tricine gels (Jimenez-Huete *et al*., 1998). In each experiment at least three samples of noninfected N2a cells were subjected to PK digestion to assure that PK-sensitive PrP^{C} was completely digested. In samples not digested with PK, which were used to estimate the absolute level of PrP in the cell lysate, the total amount of protein loaded onto the SDS-polyacrylamide was 10 μg. Following overnight electrophoresis the protein was transferred onto nitrocellulose membranes (Amersham Biosciences, Piscataway, NJ, USA) for 1 h at 400 mA using CAPS buffer (3-cyclohexylamino-1-propanesulphonic acid) containing 10% methanol. The membranes were blocked with 5% nonfat milk in TBST (Tris, 10 mM; NaCl, 150 mM; Tween 20, 0.1%, pH 7.5) for 1 h at room temperature and then incubated with Mab 6D11 diluted 1 : 3000. Following extensive washing in TBST the membranes were incubated with a horseradish peroxidase-conjugated sheep antimouse antibody (Amersham) and then developed using an

enhanced chemiluminescent substrate (SuperSignal; Pierce). Membranes were apposed to autoradiography film (X-Omat Blue XB-1; Kodak, New Haven, CT, USA). The exposure time was kept standard for all experiments at 30 s. Developed films were converted into eight-bit grayscale digital files using a Epson Perfection 4990 scanner (Epson America, Long Beach, CA, USA) and Adobe Photoshop software 7.01 (Adobe Systems, San Jose, CA, USA) and saved in a TIF format with a resolution of 600 dpi. Quantification of PrP^{Sc} was performed by densitometric analysis using NIH Image J software v. 1.34. Areas under the curves for three PrP bands representing non-, mono- and diglycosylated isoforms of the protein were summarized from each sample to calculate the total PrP level.

Mabs

Production and characterization of anti-PrP Mabs 8B4, 11G5, 7H6, 7A12, 2C2, 8H4, 8F9 and 9H7 (Table 1) have been described previously (Zanusso *et al*., 1998;Liu *et al*., 2001;Pan *et al*., 2002;2004; 2005;Wong *et al*., 2003). This set of Mabs reacts with the major structural domains of PrP. All are capable of binding both PrP^{C} and PrP^{Sc} with varying levels of affinity (Pan *et al*., 2004;Wong *et al*., 2003). 7D9 is a Mab raised against recombinant PrP (recPrP) and which recognizes a nonlinear epitope on PrP^{Sc} and PrP^{C} (Adler *et al*., 2003;Sadowski *et al*., 2003). 6D11 is a novel Mab raised against a nondenaturated PK-resistant fragment of PrP^{Sc} which has been purified from brains of CD-1 mice infected with the 139A mouse-adapted scrapie agent according to previously published protocols (Kascsak *et al*., 1986;Carp *et al*., 2000). Immunization of $Prnp^{0/0}$ mice, isolation of splenocytes and their immortalization by fusion to myeloma cells, and identifications of clones by ELISA were performed using routine protocols (Kascsak *et al*., 1987;Zanusso *et al*., 1998). Binding of 6D11 to PrP^{C}, recPrP, PK-resistant PrP^{Sc} fragments from brain homogenates and N2a/22L cell lysates was tested using Western blot as described above. Characterization of the 6D11 binding epitope was performed using a dot–blot assay. Thirty-mer peptides spanning the sequence of the PK-resistant PrP^{Sc} fragment (PrP residues 93–229) were synthesized at the W. M. Keck Foundation Facility (Yale University, New Haven, CT, USA) by solid-phase technique and purified by reverse-phase liquid chromatography, and their mass and purity were assessed by mass spectrometry (Sigurdsson *et al*., 2001;Sigurdsson *et al*., 2002a;Sadowski *et al*., 2004a). The peptides (0.3, 0.6, 1.2 and 1.8 μg/well) were blotted onto Immobilon PVDF membrane (Millipore Corporation, Billerica, MA, USA). Full-length recPrP (manufactured as described previously; Wong *et al*., 2003) and unrelated peptides Aβ1–40 and Aβ12–28 (Sadowski *et al*., 2004a) were used as positive and negative controls, respectively. Blocking, immunoblotting and development of the dot–blot were performed as described above.

The binding affinities of Mabs were compared using a solid-phase binding assay. ELISA plates (Immulon 2 HB; Canadawide Scientific, Ottawa, ON, USA) were coated overnight with recPrP (50 ng/well) and then blocked with Superblock (Pierce) for 2 h prior to adding Mabs. Binding with the primary antibody using dilutions ranging from 12×10^{-12} to 12×10^{-9}M was performed at room temperature for 2 h, and was followed by adding rabbit antimouse IgG horseradish peroxidase-conjugated secondary antibody 1 : 3000 (Amersham). The color reaction was developed using 3,3′,5,5′-tetramethylbenzidine and stopped by adding 2 M sulphuric acid. The absorbance was measured at wavelength 450 nM. Experiments were run in triplicate. Data were fitted into a one-site binding curve, and the K_D was calculated using GraphPad Prism Software v4.03 (GraphPad Prism Software, Inc., San Diego, CA, USA).

Treatment of N2a/22L cells with Mabs

N2a/22L cells (from the fifth passage after infection and higher) were plated in six-well plates and cultured until they reached 70–80% confluence. The therapeutic efficacy of Mabs was assessed by culturing N2a/22L cells in the presence of antibodies at a concentration 10 μg/mL for 96 h. The level of PK-resistant PrP^{Sc} was measured in Western blots as described above.

Each Mab was tested in three independent experiments using independently infected cell lines. Each experiment included both a positive control (nontreated N2a/22L cells) and a negative control (N2a cells); both controls were subjected to PK digestion. The levels of PrP^{Sc} were expressed as percentages of the average value from a positive control (nontreated N2a/22L cells), whereas the optic density of the background was taken from negative control lanes (N2a cells). The effect of various Mabs was analysed using one-way ANOVA followed by a Dunnett *post hoc* test (Graph Pad Prism Software, v4.03).

Fifty per cent of maximal inhibitory concentration (IC_{50}) was established by growing N2a/22L cells in the presence of increasing concentrations of Mabs for 96 h. The PrP^{Sc} level was then measured and data were fitted in a sigmoidal dose–response curve using Graph Pad Prism Software (v4.03). Experiments were performed in triplicate.

In experiments designed to check whether treatment with Mabs resulted in a persistent abrogation of PrP^{Sc} in treated cells, N2a/22L cells were cultured in the presence of Mabs (10 μg/mL) for 8 days, changing the medium every other day. Cells were then cultured in the absence of Mabs for an additional 14 days, harvested and lysed, and the level of PrPSc was measured in cell lysates as described above.

Total PrP levels (PrP^{C} + PrP^{Sc}) and levels of β-actin and Thy-1 in N2a/22L cells treated with Mabs were measured in PK-nontreated samples. Following gel electrophoresis and Western blotting, membranes were probed with either 6D11, mouse antiβ-actin Mab (1 : 1000; Abcam, Cambridge, MA, USA) or AS02 Mab (1 : 1000; Calbiochem, CA, USA) recognizing mouse Thy-1 protein. For detection of Thy-1 protein the electrophoresis was performed under nonreducing conditions, according to the manufacturer's recommendations. Densitometric measurement was performed as described above and the optic densities are expressed as percentages of the average protein level of nontreated N2a/22L cells. Experiments were performed in triplicate. Values were compared using one-way ANOVA followed by Dunnett's *post hoc* test. The β-actin is a structural 43-kDa protein (Shashidhar *et al*., 2005), unrelated to PrP^{Sc} pathological biology, and was used as a marker of general protein expression in treated cells (Korth *et al*., 2001; Perrier *et al*., 2004). Thy-1 is a 31-kDa glycosylphosphatidylinositol-anchored protein, abundantly expressed by neurons, which coexists with PrP^{C} on the external plasma membrane surface and shares similarities in trafficking and metabolism (Tiveron *et al*., 1994; Madore *et al*., 1999; Sunyach *et al*., 2003).

The cytotoxicity of anti-PrP Mabs was tested by culturing N2a and N2a/22L cells in 96-well microtiter plates in the presence of 10 μg/mL Mabs for 96 h. Following completion of treatment, the viability of cells was assessed using a colorimetric 3-(4,5-dimethylthiazol-2-yl)2,5-diphenyltetrazolium bromide (MTT) assay (Roche) performed according to the manufacturer's instructions (Sadowski *et al*., 2004a; Sigurdsson *et al*., 2001). The viability of cells treated with various Mabs, murine IgG and nontreated control cells were compared using one-way ANOVA followed by a Dunnett *post hoc* test.

In vivo PrP labeling was performed in N2a and N2a/22L cells using Mab 6D11 conjugated with Cy3 fluorescent dye (6D11/Cy3). 6D11 was conjugated with Cy3 using a Pierce antibody labeling kit applied according to the manufacturer's instructions. Cells were cultured on coverslips placed in 10-cm^2 wells in the presence of 10 μg/mL 6D11/Cy3 for 12, 24, 48 or 72 h, fixed with 20% ice-cold methanol, counterstained with DAPI (4′,6-diamidino-2-phenylindole dihydro-chloride) and analysed under a deconvolution fluorescence microscope Zeiss Axioskop 40 (Carl Zeiss AG, Gottingen, Germany) or a Bio-Rad (Hercules, CA, USA) Radiance 2000 confocal system attached to the Olympus BX50WI fluorescence microscope.

Prevention of N2a infection with Mabs

In experiments designed to prevent infection, N2a cells were cultured overnight in six-well plates with 10 μg/mL of Mabs in 2 mL of MEM. After washing with phosphate-buffered saline, cells were infected with 22L brain homogenates as described above. In similar experiments 2% brain homogenates diluted in 1 mL of Opti-MEM was incubated with 20 μg Mabs for 2 h and then used to infect cells. The PrP^{Sc} levels were measured in subsequent passages and compared to the level of PrP^{Sc} in N2a/22L cells infected simultaneously without preincubation with Mabs. Differences between control and treated groups were compared using repeated-measures ANOVA (Statistica v6.1; StatSoft Inc, Tulsa, OK, USA).

In addition we performed an animal experiment to ascertain whether prophylactic treatment with Mabs administered immediately following prion exposure may delay the onset of neurological symptoms. Two cohorts of 3-month-old male CD-1 mice, 20 animals each, were inoculated by intraperitoneal injection of 100 μL of 10% brain homogenate from terminally sick 22L-infected mice (Sigurdsson *et al*., 2002a; Sadowski *et al*., 2003; Sadowski *et al*., 2004b). An hour after exposure one cohort received intravenous infusion of murine IgG and the other cohort received Mab 7D9. Selection of this particular Mab was dictated by its effectiveness in the prevention of infection in cell culture as well as its availability in large quantities. Starting from the beginning of the 4th month following inoculation mice were tested for the first symptoms of prion infection using an apparatus containing a series of parallel bars (3 mm in diameter) placed 7 mm apart. The earliest detectable clinical symptoms of central nervous system involvement include an impaired activity level and competency when mice attempt to cross a series of parallel bars. An animal was considered clinically symptomatic if it scored positive for disease for 3 weeks in a row by an observer blinded to the animal's treatment group assignment. Upon receiving the third positive score in a row, an animal was killed with an overdose of pentobarbital (150 mg/kg body weight) and the clinical diagnosis was confirmed by demonstration of PrP^{Sc} on Western blot from PK-digested brain homogenate. This method of scoring in prion-infected mice for early detection of neurological symptoms has been validated and widely used by the authors previously (Sadowski *et al*., 2003; Sigurdsson *et al*., 2002b; Sigurdsson *et al*., 2003). Data were analysed using Kaplan–Meier survival curves followed by a log rank test. Analysis was performed using GraphPad Prism Software.

Results

6D11 is a highly sensitive Mab recognizing PrP^{C}, PrP^{Sc} and recPrP. Western blot studies demonstrated that 6D11 reacted equally well with both PrP^{C} and PrP^{Sc}, recognizing all three isoforms: di-, mono- and nonglycosylated (Fig. 1). 6D11 also recognized recPrP. Solid-phase binding studies showed that the affinity of 6D11 for PrP is higher than that of other Mabs (Table 1). The K_D value calculated for 6D11 ($8.5 \pm 0.18 \times 10^{-11}$ M) was about one-half that calculated for 7A12 and ~40 and 125 times lower than those calculated for 2C2 and 8F9, respectively. However, the binding affinities of the other Mabs used in this study are in a similar range (Table 1).

Antigen mapping studies demonstrated that 6D11 reacted with a synthetic peptide homologous to PrP residues 93–122 but showed no reaction with a peptide spanning residues 109–141, which indicates that 6D11 epitope is localized between position 93 and 109. In a dot–blot experiment, 6D11 reacted with similar affinity with PrP 93–122 as it did with full-length recPrP. This was further confirmed by an ELISA experiment, where the K_D of 6D11 binding to PrP 93–122 ($15.5 \pm 0.24 \times 10^{-11}$ M) was found to be similar to that calculated for its binding to recPrP.

22L mouse-adapted scrapie strain induced PrP^{Sc} formation in the N2a cell line

Exposure of N2a murine neuroblastoma cells to brain homogenate from terminally sick CD-1 mice infected with 22L mouse-adapted scrapie strain resulted in stable infection of this cell line. A high level of PK-resistant PrP^{Sc} could be demonstrated in subsequent passages (Fig. 2A) and N2a/22L cells divided vigorously for 12–14 passages after infection. A decreased mitotic rate and inefficient growth was routinely observed in passages higher than the 12th.

As has been described previously, wild-type N2a cells are resistant to infection with many other mouse-adapted scrapie strains including 87V, 139A and ME7 (Bosque & Prusiner, 2000). Infectivity with 139A has only been reported in transfected N2a cells overexpressing PrP^{C} (Nishida *et al.*, 2000). Therefore, we used 87V, 139A and ME7 strains as a negative control for the infection experiment to differentiate between inoculum-derived PrP^{Sc} and PrP^{Sc} formed *de novo* from PrP^{C} expressed by N2a cells. As demonstrated in Fig. 2B, only exposure to the 22L strain resulted in the stable infection and sustained formation of PK-resistant PrP^{Sc} derived from PrP^{C} expressed by the N2a cells. For comparison, exposure to 87V, 139A or ME7 produced a weak PrP^{Sc} signal seen in the first passage, which almost completely faded out in the second passage. No PrP^{Sc} could be detected in the third and higher passages.

Treatment of N2a/22L cells with 6D11, 7H6 and 7A12 Mabs abrogated the presence of PrP^{Sc}

Culturing of N2a/22L cells in the presence of Mabs produced variable lowering of the PrP^{Sc} level (Fig. 3). Three Mabs, 6D11, 7H6 and 7A12, were found capable of complete abrogation of the PrP^{Sc} presence in N2a/22L cells. Among these Mabs, 6D11 showed the lowest IC_{50} (Fig. 4). It was calculated from a sigmoidal dose–responese curve to be 0.07 ± 0.009 μg/mL (0.47 ± 0.06 μM; mean ± SD from at least three independent experiments). Values of IC_{50} for 7H6 and 7A12 were 0.16 ± 0.02 μg/mL (1.07 ± 0.13 μM) and 0.35 ± 0.05 μg/mL (2.35 ± 0.34 μM), respectively. The treatment effect of these Mabs was persistent as when antibodies were removed from the medium and the cells were grown for another 14 days in antibody-free medium no PrP^{Sc} was be detected (Fig. 5).

A significant reduction in PrP^{Sc} levels was observed with treatment using the following Mabs: 8H4 (reduction in PrP^{Sc} level by 76.6%, $P < 0.001$), 11G5 (76% reduction, $P < 0.001$), 8B4 (54% reduction, $P < 0.01$) and 2C2 (33.9% reduction, $P < 0.05$; Fig. 3). No significant effect on PrP^{Sc} levels in N2a/22L cells was observed with treatment using Mabs 7D9, 9H7 or 8F9, or murine IgG. Thus, as all of these Mabs specifically bind PrP with similar affinity, another antibody-specific parameter is required to affect the PrP^{Sc} level.

Mabs did not lower the total PrP or β-actin levels but altered the level of Thy-1

To evaluate whether the therapeutic effect of Mabs was mediated by the suppression of PrP^{C} level the total PrP level was measured in N2a/22L cells treated with Mabs. Cell lysates were divided into fractions treated and not treated with PK; these were then subjected to electrophoresis and immunoblotting to measure the levels of PrP^{Sc} and total PrP, respectively. While treatment with Mabs such as 2C2 resulted in a partial reduction in PrP^{Sc} and treatment with Mabs such as 6D11 and 7H6 completely blocked PrP^{Sc} formation, the level of total PrP under treatment with these Mabs was similar to that of nontreated N2a/22L cells (Figs 6 and 7). While comparing the density of immunoblots for PK-treated and -nontreated samples one has to keep in mind that PK-nontreated samples contained 10 μg of protein from cell lysate, whereas 200 μg of protein was subjected to PK digestion prior to loading on the gel to give bands of similar intensity. Therefore, we estimate that PrP^{Sc} constituted 5% of the total PrP. We showed that blocking PrP^{Sc} formation did not affect the total PrP signal significantly. As

the total PrP signal corresponded mainly to PrP^C, we suggest that that the therapeutic effect of our Mabs did not appear to be mediated via alteration of the PrP^C level.

To assess whether treatment with Mabs affected expression of other proteins, we quantified the level of β-actin and Thy-1. β-Actin is a 43-kDa structural protein unrelated to PrP metabolism (Shashidhar *et al*., 2005), and is commonly used as marker of general protein expression in cell culture treatment experiments (Korth *et al*., 2001; Perrier *et al*., 2004). Thy-1, however, colocalizes with PrP^C on the external plasma membrane surface and to a great extent shares endocytosis and trafficking pathways (Tiveron *et al*., 1994; Madore *et al*., 1999; Sunyach *et al*., 2003). We did not detect differences in the β-actin level between treated and nontreated N2a/22L cells (Figs 6C and 7). However, the level of Thy-1 was increased in infected cells and returned to control levels when infected cells were treated with therapeutically effective Mabs. Mabs which did not have a significant effect on PrP^{Sc} formation, such as 7D9 and 8F9, did not alter the level of Thy-1 compared to nontreated N2a/22L cells (Fig. 8A and B). As the level of Thy-1 in N2a/22L cells was over twice that in noninfected cells ($P < 0.01$), its reduction appears to be associated with a treatment effect rather than indicating cellular toxicity.

Mabs were not toxic

Potential toxicity related to treatment with anti-PrP Mabs in cells expressing PrP^C and in those actively forming PrP^{Sc} was also specifically assessed using the MTT metabolic assay. Both N2a and N2a/22L cells were grown in the presence of anti-PrP Mabs and IgG as a nonspecific control in conditions similar to those used in treatment experiments. A minor trophic effect was observed in N2a cells. Viability of N2a cells was increased by 25–35% of control values ($P < 0.01$; Fig. 9A). This trophic effect did not appear to be specific as a similar increase in N2a cell viability was observed when these cells were grown in the presence of murine IgG. N2a/22L cells cultured in the presence of anti-PrP Mabs or murine IgG did not show either trophic or toxic effects (Fig. 9B).

Measuring protein expression served also as an indirect test to assess the toxicity of Mabs. In addition to specifically measuring the β-actin level, the total protein amount in cell lysates was always calculated and compared between treated and nontreated cells to monitor for potential toxicity. The total protein amount harvested from a confluent 10-cm^2 well containing N2a/22L cells ranged between 350 and 500 μg.

Mab 6D11 was internalized by N2a/22L cells

In order to better understand how anti-PrP Mabs clear infected N2a/22Lcells of PrP^{Sc}, N2a and N2a/22L cells were cultured in the presence of Cy3-labeled Mab 6D11. N2a cells showed distinct labeling of the cytoplasmic membrane with only modest intracellular penetration of the dye despite an incubation period extended to 72 h (Fig. 10A and C). Images obtained using confocal microscopy confirmed that the labeling pattern was consistent with binding of 6D11/Cy3 to PrP^C expressed primarily on the outer surface of plasma membrane (Fig. 10E, arrowhead). In addition to labeling the cytoplasmic membrane, N2a/22L cells showed internalization of 6D11/Cy3 and their accumulation in the cytoplasm which continued over the time of experiment (Fig. 9B, D and E).

Mabs reduced prion infectivity

Both preincubation of N2a cells prior to inoculation and preincubation of the brain homogenate from 22L-infected mice with anti-PrP Mabs resulted in significantly decreased levels of PrP^{Sc} in subsequent passages compared to N2a cells infected in the standard way (Fig. 11). In the third passage, the PrP^{Sc} level was reduced by 74% when the inoculum was preincubated with 6D11 Mab, and by 84% when the N2a cells were exposed to 6D11 prior to the infection

(Fig. 11A; $P < 0.01$). The PrP^{Sc} level was followed in subsequent passages and it continued to be significantly reduced. The reduction ranged from 4 to 41% of the PrP^{Sc} level in control N2a/22L cells in passages 3–7 (Fig. 11B; repeated-measures ANOVA; $P < 0.001$). Mab 7D9, which did not have therapeutic efficacy in lowering PrP^{Sc} levels in already infected N2a/22L cells, showed a surprising and significant preventive effect in that it reduced the PrP^{Sc} level by 88.5% ($P < 0.01$) and by 57% ($P < 0.05$) when it was incubated with the inoculum and with N2a cells, respectively (Fig. 11A). Mab 7A12, which was capable of completely blocking PrP^{Sc} formation in already infected N2a/22L cells, showed the weakest preventive effect. In the third passage, the PrP^{Sc} level was reduced by only 41 and 43% ($P < 0.05$), respectively, when the inoculum and N2a cells were preincubated with 7A12 (Fig. 11A). In the subsequent passages, the PrP^{Sc} level in the experiments with 7A12, but not with 6D11 or 7D9, gradually increased and in the sixth passage was not significantly different from that in control N2a/22L cells.

To evaluate whether this preventive effect of Mabs was also relevant *in vivo* we administered a single dose of 7D9 Mab to CD-1 mice within 1 h following intraperitoneal inoculation with infectious brain homogenate. The selection of 7D9 was based upon the availability of large amounts of this Mab required for the experiment and its effectiveness in tissue culture studies. The Kaplan–Meier survival analysis demonstrated a statistically significant treatment effect. The difference between the median incubation period for groups treated with Mab 7D9 and murine IgG was 28 days (Fig. 12; $P < 0.0001$, log rank test).

Discussion

Using a panel of Mabs directed against the major structural domains of PrP we demonstrated that a number of Mabs inhibit PrP^{Sc} formation by an antigen-specific disruption of the PrP^{C}–PrP^{Sc} interaction. Three Mabs, 6D11, 7H6 and 7A12, were found to be capable of completely eradicating PrP^{Sc} from infected N2a cells. Mabs 7H6 and 7A12 bind to neighbouring epitopes corresponding to PrP sequences 130–140 and 143–155, respectively. The importance of the PrP 130–150 sequence, which includes the first α-helical domain (PrP residues 143–155) for the PrP^{C}–PrP^{Sc} interaction and the formation of PrP^{Sc}, has been suggested by several investigators (Enari *et al*., 2001a; Heppner *et al*., 2001; Peretz *et al*., 2001; White *et al*., 2003; Perrier *et al*., 2004). Other reports also identified the 132–156 region of the protein as critical for interspecies transmission of prionoses (Kocisko *et al*., 1995; Scott *et al*., 1993; Priola & Chesebro, 1995). Therefore, the PrP sequence 130–150 represents an important target for the development of anti-PrP drugs. Mabs 11G5 and 2C2 reacting with linear epitopes flanking downstream and upstream regions of this sequence had a partial effect in clearing PrP^{Sc}. It has been shown that PrP sequences 119–136 and 166–179, partially covered by the epitopes of these antibodies, play an auxiliary role in the PrP^{C}-to-PrP^{Sc} conversion (Horiuchi & Caughey, 1999). On the other hand, the effect of these antibodies may be due to steric hindrance. Because of their size, which is several times bigger than PrP itself, they may indirectly block access to the 130–150 domain.

6D11 is a novel Mab, raised against the PK-resistant fragments of PrP^{Sc}, which also showed an excellent effect in clearing N2a/22L cells of PrP^{Sc}. 6D11 had the highest binding affinity to recPrP among the studied Mabs and also bound robustly to PrP^{Sc}. Dot–blot experiments demonstrated that the 6D11 epitope is located between residues 93 and 109, as shown by the finding that the antibody bound with high affinity to a peptide homologous to PrP residues 93–122 and showed no binding to a peptide homologous to sequence 109–141. The localization of the major 6D11 epitope was further narrowed to residues 97–100 by pepscan assay (Pepscan Systems, Lelystad, The Netherlands; data not shown). 6D11 did not recognize the PrP 130–155 sequence as tested by dot–blot, immunoprecipitation and ELISA studies. These observations indicate that the epitope along PrP residues 93–109 is in addition to residues 130–

155, another important therapeutic target for the inhibition of PrP^{Sc} formation. Neutralization of this antigen by 6D11 may either prevent the PrP^{C}–PrP^{Sc} interaction or interfere with binding auxillary molecules essential to prion propagation (Kaneko *et al*., 1997; Hundt *et al*., 2001; Leucht *et al*., 2003).

Among other tested Mabs, a partial effect in lowering the PrP^{Sc} level could be demonstrated by using Mabs 8B4, directed against the N-terminus, and 8H4 directed against the second α-helix domain. No effect was observed with Mab 8F9 reacting against a linear epitope on the C-terminus of PrP. These observations are consistent with our *in vivo* observation where symptoms of prion disease were delayed in mice treated with Mabs 8H4 and 8B4 but not 8F9 (Sigurdsson *et al*., 2003). No significant effect on PrP^{Sc} level in N2a/22L cells was observed following treatment with Mabs 7D9, 9H7 or 8F9, nor with murine IgG. Similarly, Feraudet *et al*. (2005), who analysed the therapeutic efficacy of 145 Mabs raised against different forms of human, ovine, hamster and murine PrP, demonstrated that a partial treatment response can be achieved with Mabs directed against epitopes located outside the central potion of the PrP sequence. However, the most effective Mab in their study, Sha 31, reacted with an epitope located along residues 145–152 which is similar to the epitope of our 7A12 Mab.

All Mabs used had high binding affinity to the PrP, and this appears to be a prerequisite for therapeutic effectiveness. The K_D of binding to PrP for all Mabs used in this study was within the picomolar range as analysed by solid-phase binding assays. The exceptions were Mabs 2C2 and 8F9, which showed slightly higher K_D values. As all investigated Mabs specifically bound PrP with closely similar affinity, this feature does not appear to be a primary parameter determining their therapeutic efficacy. Furthermore, 2C2, which had a K_D ~40× higher than that of 6D11 and 15× higher than that of 7H6, showed only partial therapeutic effects in N2a/22L cells whereas Mabs 7D9 and 9H7, with binding affinities to PrP ~4× and 3× better, respectively, than that of 2C2 were completely ineffective. Therefore, differences in binding affinity cannot in and of themselves account for their disparate therapeutic effects. Although it is desirable for a therapeutic antibody to have the highest affinity possible, this property appears to be of secondary importance to their targeting of specific critical PrP domains.

The interaction of PrP^{Sc} with PrP^{C}, and the replication of PrP^{Sc}, take place both on the cell surface and in the cytosol (DeArmond *et al*., 2002). When N2a/22L cells were incubated with 6D11/Cy3 Mabs, initial labeling of cell membranes was followed by internalization of antibodies and their accumulation in the cytosol. Internalization of Mabs was minimal in noninfected N2a cells. These observations indicate that 6D11 binds PrP^{Sc} and is internalized together with PrP^{Sc}. Therefore, it can prevent the PrP^{Sc}–PrP^{C} interaction not only on the cell membrane surface but also within the cytoplasm, preventing lysosomal and cytoplasmic accumulation and formation of new PrP^{Sc} (Ma & Lindquist, 2002; Ma *et al*., 2002).

Toxicity is a potential adverse effect associated with immunization approaches. Autoimmune meningoencephalitis occurring in 6% of patients resulted in premature termination of a clinical trial of an Alzheimer's vaccine (Nicoll *et al*., 2003; Orgogozo *et al*., 2003). Passive immunization is less likely to initiate an uncontrolled autoimmune reaction (Schenk, 2002; Sadowski & Wisniewski, 2004), but Mabs targeting PrP^{Sc} formation *in vivo* must not exert toxicity toward cells replicating PrP^{Sc} and at the same time expressing PrP^{C}. One of the previous studies analysing the effects of anti-PrP Mabs on PrP^{C} metabolism in noninfected cells suggested that the anti-PrP Mabs may shorten the PrP^{C} half-life and thus their therapeutic effect is related to depletion of PrP^{C} (Perrier *et al*., 2004). However, in a follow-up study the same group reported contradictory results, showing that Mabs do not lower PrP^{C} level in infected cells (Feraudet *et al*., 2005). In view of our data, anti-PrP Mabs which effectively abrogate PrP^{Sc} infection do not appear to lower PrP^{C} level. In addition we investigated the effect of treatment on the level of two proteins, β-actin and Thy-1. Interestingly, we found the

level of Thy-1 in N2a/22L cells to be over twice that in noninfected cells. As Thy-1 and PrP coexist in close proximity on the outer surface of the plasma membrane and share similarities in trafficking and metabolism (Madore *et al*., 1999; Sunyach *et al*., 2003), an increased level of Thy-1 appears to be related to the infectious status of the N2a cells. Whether this is a result of its overexpression or extended half-life remains yet to be elucidated. Nevertheless in N2a/22L cells cultured in the presence of therapeutically active anti-PrP Mabs, the Thy-1 level is reduced to a level similar to noninfected cells. This appears to be additional evidence demonstrating the therapeutic effect of our Mabs. The level of β-actin, which is a structural protein not involved in the PrP^{C}–PrP^{Sc} interaction, is unchanged during treatment. This suggests that our Mabs do not affect general protein expression. The MTT cytotoxicity assay also demonstrated a lack of Mab toxicity in both N2a/22L and N2a cells.

Preincubation of the inoculum with several Mabs resulted in a significant decrease in its infectivity as the Mabs bind and neutralize PrP^{Sc}. Likewise, the level of PrP^{Sc} formation was effectively decreased when N2a cells were preincubated with several different Mabs. Previous experiments demonstrated that Mabs which preferentially bind PrP^{C} may also successfully clear infected cell cultures by sequestering PrP^{C} on the cell membrane (Enari *et al*., 2001b; Kim *et al*., 2004; Feraudet *et al*., 2005). However, in animal experiments Mabs which equally recognize PrP^{Sc} and PrP^{C} appeared to be more effective (White *et al*., 2003). In experiments with 6D11/Cy3 we were able to directly demonstrate that Mabs bind to PrP^{C} on the membrane surface of noninfected cells. Thus, sequestration of PrP^{C} on the cell surface by Mabs and inhibition of its contact with PrP^{Sc} from the inoculum has a strong protective effect against infection. No epitope-specific effect was observed in experiments designed to prevent infection. Mab 7D9, which showed no therapeutic effect in reducing PrP^{Sc} level in N2a/22L cells, was more effective than Mab 7A12 which produced persistent abrogation of PrP^{Sc} infection. Only Mab 6D11, which had the strongest therapeutic effect in N2a/22L cells, was also effective in preventing infection. These experiments illustrate additional therapeutic mechanisms of anti-PrP Mabs which appear to be relevant to *in vivo* treatment as demonstrated in an experiment where mice were treated with a single dose of 7D9 shortly after exposure. These treated mice showed a significantly prolonged symptom-free incubation period.

The therapeutic mechanisms of anti-PrP Mabs which include: (i) antigen-specific interference of PrP^{C}–PrP^{Sc} interaction; (ii) PrP^{Sc} neutralization; and (iii) PrP^{C} sequestration on the cell surface, are not mutually exclusive but may synergistically potentiate the therapeutic effects of Mabs. All three mechanisms should be considered in the development of therapeutic strategies, mindful that the disease process in a living organism is far more complex than that in infected cell lines. In animal or human diseases, the formation of PrP^{Sc} in already-infected cells occurs concurrently with a constant process of infecting other cells (Weissmann *et al*., 2002). Therefore, the ability of Mabs to reduce prion infectivity is desirable in addition to their primary function, which is antigen-specific blocking of PrP^{Sc} formation. 6D11 is an example of an antibody with all three properties. Our studies demonstrate that anti-PrP Mabs constitute a safe and feasible therapeutic approach for the treatment of prion infections. Information regarding antigen-specific inhibition of PrP^{Sc} formation is important for the rational design of humoral therapy for prion infection in animals and eventually in humans.

Acknowledgements

Supported by AG24847 (M.S.), NS47433 (T.W.), AG15408 (T.W.), NS45981 (M.S.S.), US Department of Army contract (DAMD17-03-1-0286 (M.S.S.) and NIH contract N01-NS-02327 (R.J.K.).

References

Adler V, Zeller B, Kryukov V, Kascsak R, Rubenstein R, Grossman A. Small, highly structured RNAs participate in the conversion of human recombinant Prp (Sen) to Prp (Res) in vitro . J Mol Biol 2003;332:47–57. [PubMed: 12946346]

Balter M. Spongiform disease. Experts downplay new vCJD fears. Science 2002;289:1866–1867. [PubMed: 11012352]

Bosque PJ, Prusiner SB. Cultured cell sublines highly susceptible to prion infection. J Virol 2000;74:4377–4386. [PubMed: 10756052]

Carp RI, Meeker HC, Rubenstein R, Sigurdarson S, Papini M, Kascsak RJ, Kozlowski PB, Wisniewski HM. Characteristics of scrapie isolates derived from hay mites. J Neurovirol 2000;6:137–144. [PubMed: 10822327]

DeArmond, SJ.; Kretzschmar, H.; Prusiner, SB. Prion diseases. In: Graham, DI.; Lantos, P., editors. Greenfield's Neuropathology. Arnold; London: 2002. p. 273-324.

Eklund CM, Kennedy RC, Hadlow WJ. Pathogenesis of scrapie virus infected mice. J Infect Dis 1967;117:15–22. [PubMed: 4961240]

Enari M, Flechsig E, Weissmann C. Scrapie prion protein accumulation by scrapie-infected neuroblastoma cells abrogated by exposure to a prion protein antibody. Proc Natl Acad Sci USA 2001a; 98:9295–9299. [PubMed: 11470893]

Enari M, Flechsig E, Weissmann C. Scrapie prion protein accumulation by scrapie-infected neuroblastoma cells abrogated by exposure to a prion protein antibody. Proc Natl Acad Sci USA 2001b; 98:9295–9299. [PubMed: 11470893]

Feraudet C, Morel N, Simon S, Volland H, Frobert Y, Creminon C, Vilette D, Lehmann S, Grassi J. Screening of 145 anti-PrP monoclonal antibodies for their capacity to inhibit PrPSc replication in infected cells. J Biol Chem 2005;280:11247–11258. [PubMed: 15618225]

Goni F, Knudsen E, Schreiber F, Scholtzova H, Pankiewicz J, Carp R, Meeker HC, Rubenstein R, Brown DR, Sy MS, Chabalgoity JA, Sigurdsson EM, Wisniewski T. Mucosal vaccination delays or prevents prion infection via an oral route. Neuroscience 2005;133:413–421. [PubMed: 15878645]

Heppner FL, Musahl C, Arrighi I, Klein MA, Rulicke T, Oesch B, Zinkernagel RM, Kalinke U, Aguzzi A. Prevention of scrapie pathogenesis by transgenic expression of anti-prion protein antibodies. Science 2001;294:178–182. [PubMed: 11546838]

Herzog C, Sales N, Etchegaray N, Charbonnier A, Freire S, Dormont D, Deslys JP, Lasmezas CI. Tissue distribution of bovine spongiform encephalopathy agent in primates after intravenous or oral infection. Lancet 2004;363:422–428. [PubMed: 14962521]

Hilton DA, Ghani AC, Conyers L, Edwards P, McCardle L, Penney M, Ritchie D, Ironside JW. Accumulation of prion protein in tonsil and appendix: review of tissue samples. Br Med J 2002;325:633–634. [PubMed: 12242174]

Hilton DA, Ghani AC, Conyers L, Edwards P, McCardle L, Ritchie D, Penney M, Hegazy D, Ironside JW. Prevalence of lymphoreticular prion protein accumulation in UK tissue samples. J Pathol 2004a; 203:733–739. [PubMed: 15221931]

Hilton DA, Sutak J, Smith MEF, Penney M, Conyers L, Edwards P, McCardle L, Ritchie D, Head MW, Wiley CA, Ironside JW. Specificity of lymphoreticular accumulation of prion protein for variant Creutzfeldt–Jakob disease. J Clin Pathol 2004b;57:300–302. [PubMed: 14990604]

Horiuchi M, Caughey B. Specific binding of normal prion protein to the scrapie form via a localized domain initiates its conversion to the protease-resistant state. EMBO J 1999;18:3193–3203. [PubMed: 10369660]

Houston F, Foster JD, Chong A, Hunter N, Bostock CJ. Transmission of BSE by blood transfusion in sheep. Lancet 2000;356:999–1000. [PubMed: 11041403]

Hundt C, Peyrin JM, Haik S, Gauczynski S, Leucht C, Rieger R, Riley ML, Deslys JP, Dormont D, Lasmezas CI, Weiss S. Identification of interaction domains of the prion protein with its 37-kDa/67-kDa laminin receptor. EMBO J 2001;20:5876–5886. [PubMed: 11689428]

Jimenez-Huete A, Lievens PMJ, Vidal R, Piccardo P, Ghetti B, Tagliavini F, Frangione B, Prelli F. Endogenous proteolytic cleavage of normal and disease-associated isoforms of the human prion protein in neural and non-neural tissues. Am J Pathol 1998;153:1561–1572. [PubMed: 9811348]

Kaneko K, Zulianello L, Scott M, Cooper CM, Wallace AC, James TL, Cohen FE, Prusiner SB. Evidence for protein X binding to a discontinuous epitope on the cellular prion protein during scrapie prion propagation. Proc Natl Acad Sci USA 1997;94:10069–10074. [PubMed: 9294164]

Kascsak RJ, Rubenstein R, Merz PA, Carp RI, Robakis NK, Wisniewski HM, Diringer H. Immunological comparison of scrapie-associated fibrils isolated from animals infected with four different scrapie strains. J Virol 1986;59:676–683. [PubMed: 2426470]

Kascsak RJ, Rubenstein R, Merz PA, Tonna-DeMasi M, Fersko R, Carp RI, Wisniewski HM, Diringer H. Mouse polyclonal and monoclonal antibody to scrapie-associated fibril proteins. J Virol 1987;61:3688–3693. [PubMed: 2446004]

Kim CL, Karino A, Ishiguro N, Shinagawa M, Sato M, Horiuchi M. Cell-surface retention of PrPC by anti-PrP antibody prevents protease-resistant PrP formation. J Gen Virol 2004;85:3473–3482. [PubMed: 15483265]

Kocisko DA, Priola SA, Raymond GJ, Chesebro B, Lansbury PT Jr, Caughey B. Species specificity in the cell-free conversion of prion protein to protease-resistant forms: a model for the scrapie species barrier. Proc Natl Acad Sci USA 1995;92:3923–3927. [PubMed: 7732006]

Korth C, May BC, Cohen FE, Prusiner SB. Acridine and phenothiazine derivatives as pharmacotherapeutics for prion disease. Proc Natl Acad Sci USA 2001;98:9836–9841. [PubMed: 11504948]

Leucht C, Simoneau S, Rey C, Vana K, Rieger R, Lasmezas CI, Weiss S. The 37 kDa/67 kDa laminin receptor is required for PrPSc propagation in scrapie-infected neuronal cells. EMBO Reports 2003;4:290–295. [PubMed: 12634848]

Liu T, Zwingman T, Li R, Pan T, Wong BS, Petersen RB, Gambetti P, Herrup K, Sy MS. Differential expression of cellular prion protein in mouse brain as detected with multiple anti-PrP monoclonal antibodies. Brain Res 2001;896:118–129. [PubMed: 11277980]

Ma JY, Lindquist S. Conversion of PrP to a self-perpetuating PrPSc-like conformation in the cytosol. Science 2002;298:1785–1788. [PubMed: 12386336]

Ma JY, Wollmann R, Lindquist S. Neurotoxicity and neurodegeneration when PrP accumulates in the cytosol. Science 2002;298:1781–1785. [PubMed: 12386337]

Madore N, Smith KL, Graham CH, Jen A, Brady K, Hall S, Morris R. Functionally different GPI proteins are organized in different domains on the neuronal surface. EMBO J 1999;18:6917–6926. [PubMed: 10601014]

Nicoll JAR, Wilkinson D, Holmes C, Steart P, Markham H, Weller RO. Neuropathology of human Alzheimer disease after immunization with amyloid-beta peptide: a case report. Nat Med 2003;9:448–452. [PubMed: 12640446]

Nishida N, Harris DA, Vilette D, Laude H, Frobert Y, Grassi J, Casanova D, Milhavet O, Lehmann S. Successful transmission of three mouse-adapted scrapie strains to murine neuroblastoma cell lines overexpressing wild-type mouse prion protein. J Virol 2000;74:320–325. [PubMed: 10590120]

Orgogozo JM, Gilman S, Dartigues JF, Laurent B, Puel M, Kirby LC, Jouanny P, Dubois B, Eisner L, Flitman S, Michel BF, Boada M, Frank A, Hock C. Subacute meningoencephalitis in a subset of patients with AD after A beta 42 immunization. Neurology 2003;61:46–54. [PubMed: 12847155]

Pan T, Li RL, Kang SC, Pastore M, Wong BS, Ironside J, Gambetti P, Sy MS. Biochemical fingerprints of prion diseases: scrapie prion protein in human prion diseases that share prion genotype and type. J Neurochem 2005;92:132–142. [PubMed: 15606903]

Pan T, Li RL, Kang SC, Wong BS, Wisniewski T, Sy MS. Epitope scanning reveals gain and loss of strain specific antibody binding epitopes associated with the conversion of normal cellular prion to scrapie prion. J Neurochem 2004;90:1205–1217. [PubMed: 15312175]

Pan T, Li RR, Wong BS, Liu T, Gambetti P, Sy MS. Heterogeneity of normal prion protein in two-dimensional immunoblot: presence of various glycosylated and truncated forms. J Neurochem 2002;81:1092–1101. [PubMed: 12065622]

Peden AH, Head MW, Ritchie DL, Bell JE, Ironside JW. Preclinical vCJD after blood transfusion in a PRNP codon 129 heterozygous patient. Lancet 2004;364:527–529. [PubMed: 15302196]

Peretz D, Williamson RA, Kaneko K, Vergara J, Leclerc E, Schmitt-Ulms G, Mehlhorn IR, Legname G, Wormald MR, Rudd PM, Dwek RA, Burton DR, Prusiner SB. Antibodies inhibit prion propagation and clear cell cultures of prion infectivity. Nature 2001;412:739–743. [PubMed: 11507642]

Perrier V, Solassol J, Crozet C, Frobert Y, Mourton-Gilles C, Grassi J, Lehmann S. Anti-PrP antibodies block PrPSc replication in prion-infected cell cultures by accelerating PrP degradation. J Neurochem 2004;89:454–463. [PubMed: 15056288]

Priola SA, Chesebro B. A single hamster Prp amino-acid blocks conversion to protease-resistant Prp in scrapie-infected mouse neuroblastoma-cells. J Virol 1995;69:7754–7758. [PubMed: 7494285]

Rubenstein R, Merz PA, Kascsak RJ, Scalici CL, Papini MC, Carp RI, Kimberlin RH. Scrapie-infected spleens – analysis of infectivity, scrapie-associated fibrils, and protease-resistant proteins. J Infectious Dis 1991;164:29–35. [PubMed: 1676044]

Sadowski M, Pankiewicz J, Scholtzova H, Ripellino JA, Li YS, Schmidt SD, Mathews PM, Fryer JD, Holtzman DM, Sigurdsson EM, Wisniewski T. A synthetic peptide blocking the apolipoprotein E/beta-amyloid binding mitigates beta-amyloid toxicity and fibril formation in vitro and reduces beta-amyloid plaques in transgenic mice. Am J Pathol 2004a;165:937–948. [PubMed: 15331417]

Sadowski M, Pankiewicz J, Scholtzova H, Tsai J, Li YS, Carp RI, Meeker HC, Gambetti P, Debnath M, Mathis CA, Shao L, Gan WB, Klunk WE, Wisniewski T. Targeting prion amyloid deposits in vivo. J Neuropath Exp Neurol 2004b;63:775–784. [PubMed: 15290902]

Sadowski M, Tang CY, Aguinaldo JG, Carp R, Meeker HC, Wisniewski T. *In vivo* micro magnetic resonance imaging signal changes in scrapie infected mice. Neurosci Lett 2003;345:1–4. [PubMed: 12809974]

Sadowski M, Wisniewski T. Vaccines for conformational disorders. Expert Rev Vaccines 2004;3:89–94. [PubMed: 14761246]

Schenk D. Opinion: Amyloid-beta immunotherapy for Alzheimer's disease: the end of the beginning. Nat Rev Neurosci 2002;3:824–828. [PubMed: 12360327]

Schwarz A, Kratke O, Burwinkel M, Riemer C, Schultz J, Henklein P, Bamme T, Baier M. Immunisation with a synthetic prion protein-derived peptide prolongs survival times of mice orally exposed to the scrapie agent. Neurosci Lett 2003;350:187–189. [PubMed: 14550926]

Scott M, Groth D, Foster D, Torchia M, Yang SL, DeArmond SJ, Prusiner SB. Propagation of prions with artificial properties in transgenic mice expressing chimeric Prp genes. Cell 1993;73:979–988. [PubMed: 8098995]

Shashidhar S, Lorente G, Nagavarapu U, Nelson A, Kuo J, Cummins J, Nikolich K, Urfer R, Foehr ED. GPR56 is a GPCR that is overexpressed in gliomas and functions in tumor cell adhesion. Oncogene 2005;24:1673–1682. [PubMed: 15674329]

Sigurdsson EM, Brown DR, Daniels M, Kascsak RJ, Kascsak R, Carp R, Meeker HC, Frangione B, Wisniewski T. Immunization delays the onset of prion disease in mice. Am J Pathol 2002a;161:13–17. [PubMed: 12107084]

Sigurdsson EM, Brown DR, Daniels M, Kascsak RJ, Kascsak R, Carp RI, Meeker HC, Frangione B, Wisniewski T. Vaccination delays the onset of prion disease in mice. Am J Pathol 2002b;161:13–17. [PubMed: 12107084]

Sigurdsson EM, Scholtzova H, Mehta P, Frangione B, Wisniewski T. Immunization with a nontoxic/nonfibrillar amyloid-β homologous peptide reduces Alzheimer's disease associated pathology in transgenic mice. Am J Pathol 2001;159:439–447. [PubMed: 11485902]

Sigurdsson EM, Sy MS, Li RL, Scholtzova H, Kascsak RJ, Kascsak R, Carp R, Meeker HC, Frangione B, Wisniewski T. Anti-prion antibodies for prophylaxis following prion exposure in mice. Neurosci Lett 2003;336:185–187. [PubMed: 12505623]

Sunyach C, Jen A, Deng J, Fitzgerald KT, Frobert Y, Grassi J, McCaffrey MW, Morris R. The mechanism of internalization of glycosylphosphatidylinositol-anchored prion protein. EMBO J 2003;22:3591–3601. [PubMed: 12853474]

Tiveron MC, Nostenbertrand M, Jani H, Garnett D, Hirst EMA, Grosveld F, Morris RJ. The mode of anchorage to the cell-surface determines both the function and the membrane location of Thy-1 glycoprotein. J Cell Sci 1994;107:1783–1796. [PubMed: 7983148]

UK Department of Health Monthly CJD Statistics. 2006 [Accessed on 5-May-2006]. [http://www.dh.gov.uk/PublicationsAndStatistics/PressReleases/PressReleasesNotices/fs/en]

Wadsworth JDF, Joiner S, Hill AF, Campbell TA, Desbruslais M, Luthert PJ, Collinge J. Tissue distribution of protease resistant prion protein in variant Creutzfeldt-Jakob disease using a highly sensitive immunoblotting assay. Lancet 2001;358:171–180. [PubMed: 11476832]

Weissmann C, Enari M, Klohn PC, Rossi D, Flechsig E. Transmission of prions. Proc Natl Acad Sci USA 2002;99:16378–16383. [PubMed: 12181490]

White AR, Enever P, Tayebl M, Mushens R, Linehan J, Brandner S, Anstee D, Collinge J, Hawke S. Monoclonal antibodies inhibit prion replication and delay the development of prion disease. Nature 2003;422:80–83. [PubMed: 12621436]

Wong BS, Li R, Sassoon J, Kang SC, Liu T, Pan T, Greenspan NS, Wisniewski T, Brown DR, Sy MS. Mapping the antigenicity of copper-treated cellular prion protein with the scrapie isoform. Cell Mol Life Sci 2003;60:1224–1234. [PubMed: 12861388]

Yasuhara O, Hanai K, Ohkubo I, Sasaki M, McGeer PL, Kimura H. Expression of cystatin C in rat, monkey and human brains. Brain Res 1993;628:85–92. [PubMed: 8313175]

Zanusso G, Liu DC, Ferrari S, Hegyi I, Yin XH, Aguzzi A, Hornemann S, Liemann S, Glockshuber R, Manson JC, Brown P, Petersen RB, Gambetti P, Sy MS. Prion protein expression in different species: Analysis with a panel of new mAbs. Proc Natl Acad Sci USA 1998;95:8812–8816. [PubMed: 9671761]

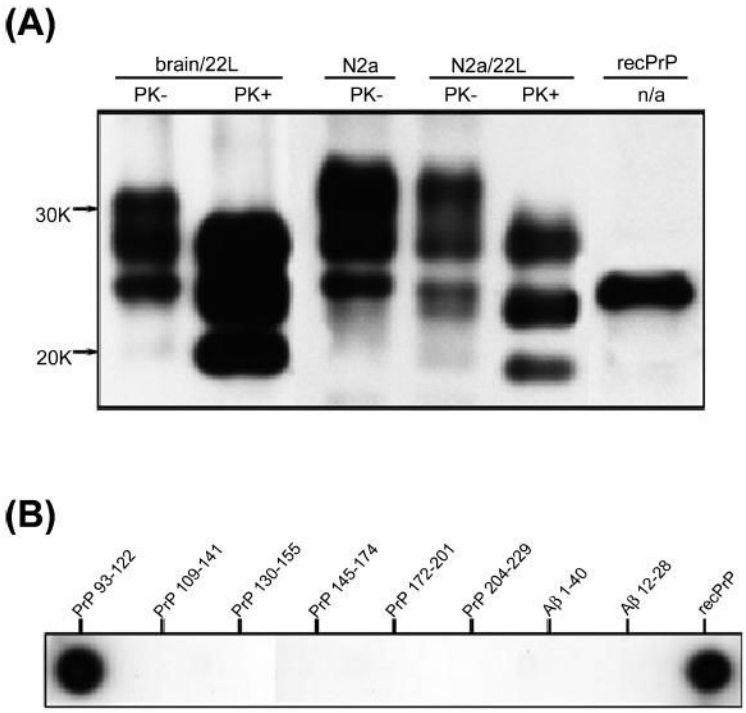

Fig. 1.

(A) Mab 6D11 detected di-, mono- and nonglycosylated PrP isoforms prior to and after PK treatment in brain homogenate from 22L-infected CD-1 mouse (brain/22L) and in cell lysate from N2a cells infected with the 22L prion strain (N2a/22L). 6D11 also reacted with PrP^{C} produced by noninfected N2a cells (N2a) and with recombinant PrP (recPrP). Ten micrograms of total protein from brain homogenate and 40 and 10 μg of total protein from cell lysates were loaded onto lanes 1, 3 and 4, respectively. Two hundred micrograms of total protein from brain homogenate or cell lysate were subjected to PK digestion and loaded onto lanes 2 and 5, and 3 μg of recPrP was loaded onto lane 6. PK-, protein not treated with PK; PK+, protein treated with PK. (B) Dot–blot analysis of 6D11 binding epitope. 6D11 reacted with a peptide homologous to PrP residues 93–122 with an affinity similar to that shown for full-length recPrP.

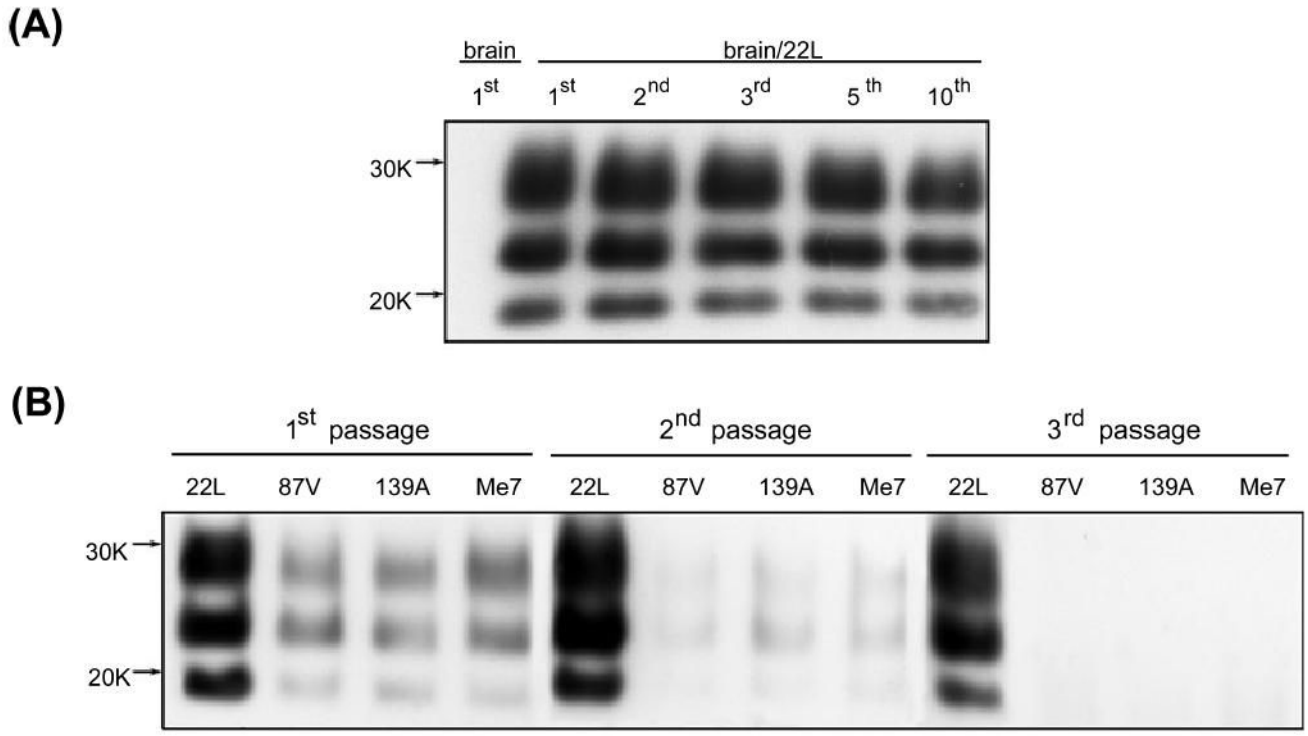

Fig. 2.

(A) PK-treated cell lysates from N2a murine neuroblastoma cells exposed to homogenate from a control brain (brain) or from a brain of a CD-1 mouse infected with 22L mouse-adapted scrapie strain (brain/22L). No PK-resistant material could be detected in cells cultured in the presence of control brain homogenate. Exposure of N2a cells to 22L mouse-adapted scrapie strain resulted in persistent infection of this line as the stable presence of PK-resistant PrP^{Sc} could be demonstrated in subsequent passages. (B) PK-treated cell lysates from N2a cells exposed to different mouse-adapted scrapie strains: 22L, 87V, 139A and ME7. Only exposure to the 22L strain resulted in the stable infection and sustained formation of PK-resistant PrP^{Sc} derived from PrP^{C} expressed by the N2a cells. A weak signal can be seen in the first passage; this almost completely fades out in the second passage and is derived either from PrP^{Sc} carried over from the inoculum or from limited, unsustained conversion of cellular PrP^{C} to PrP^{Sc}. No PrP^{Sc} could be detected in the third or higher passages of N2a cells exposed to 87V, 139A or ME7.

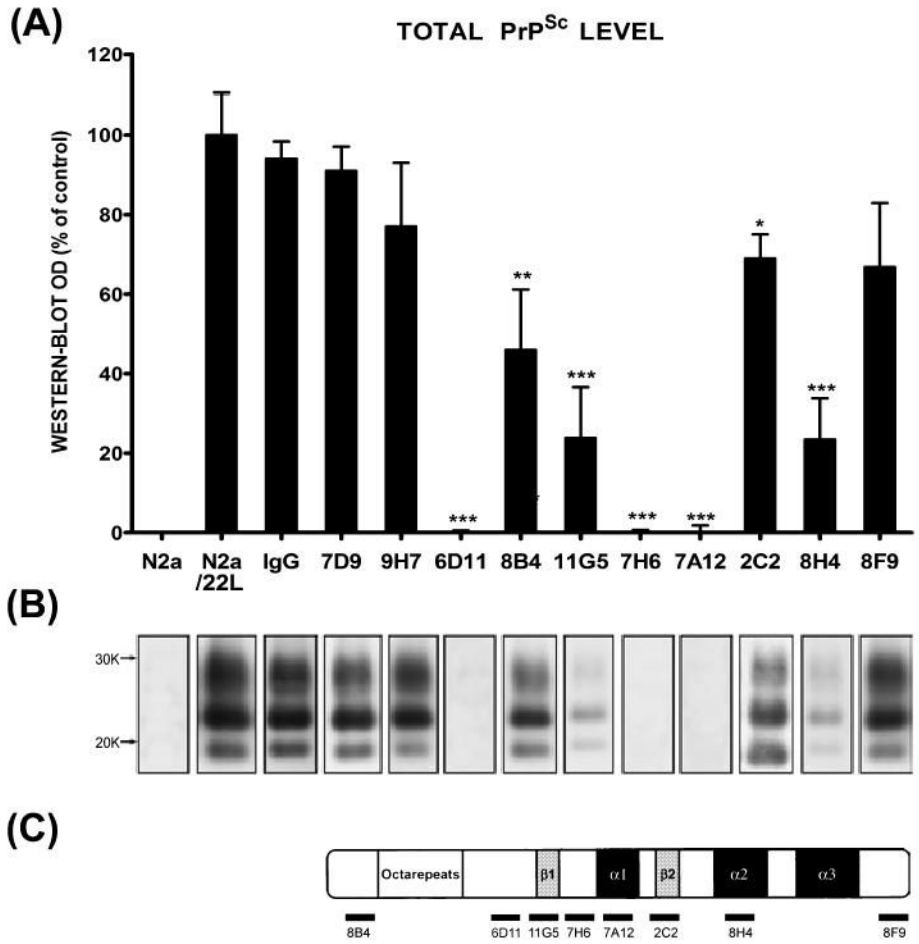

Fig. 3.

(A) The level of PrP^{Sc} in N2a/22L cells grown in the presence of anti-PrP Mabs. Mabs 6D11, 7H6 and 7A12 caused complete abrogation of PrP^{Sc} in infected cells. N2a (noninfected N2a cells), N2a/22L (N2a cells infected with the 22L strain) and IgG (N2a/22L cells incubated in the presence of murine IgG) were included as controls. OD, optical density; values are given as a mean + SD from at least three independent experiments. One-way ANOVA ($P < 0.0001$) was followed by Dunnett's *post hoc* test; *$P < 0.05$, **$P < 0.01$, ***$P < 0.001$. (B) PK-resistant PrP^{Sc} in cell lysates following treatment with particular Mabs. (C) Schematic representation of epitopes of Mabs used to treat N2a/22L cells.

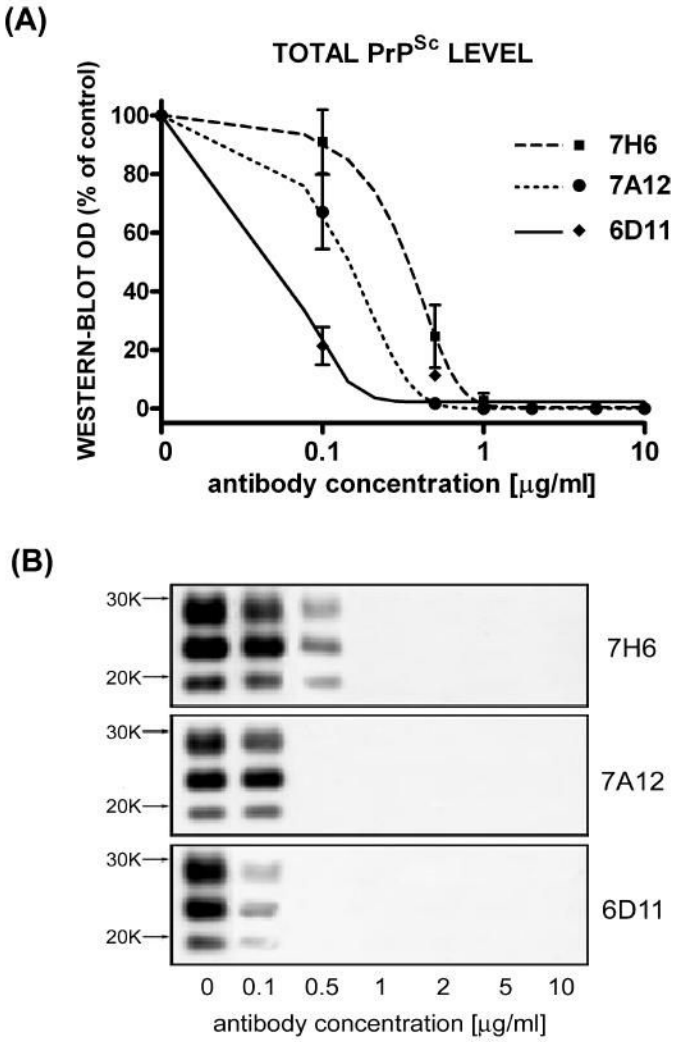

Fig. 4.

Dose-dependant inhibition of PrP^{Sc} formation in N2a/22L cells by Mabs. (A) Densitometric measurements of PrP^{Sc} bands detected in the Western blots fitted to sigmoidal dose–response curves. Values are given as mean ± SD from at least three independent experiments. (B) Western blots of PK-treated cell lysates from N2a/22L cells treated for 4 days with different concentrations of Mabs.

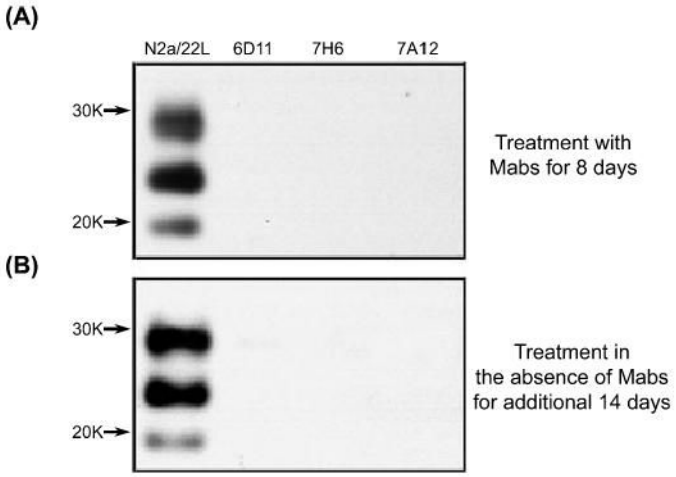

Fig. 5.

(A) Absence of PK-resistant PrP^{Sc} in N2a/22L cells incubated with Mabs 6D11, 7H6 and 7A12 for 8 days. (B) There was no reappearance of PrP^{Sc} after the cells were grown for another 14 days in the absence of Mabs. This indicates that the effect of treatment was persistent.

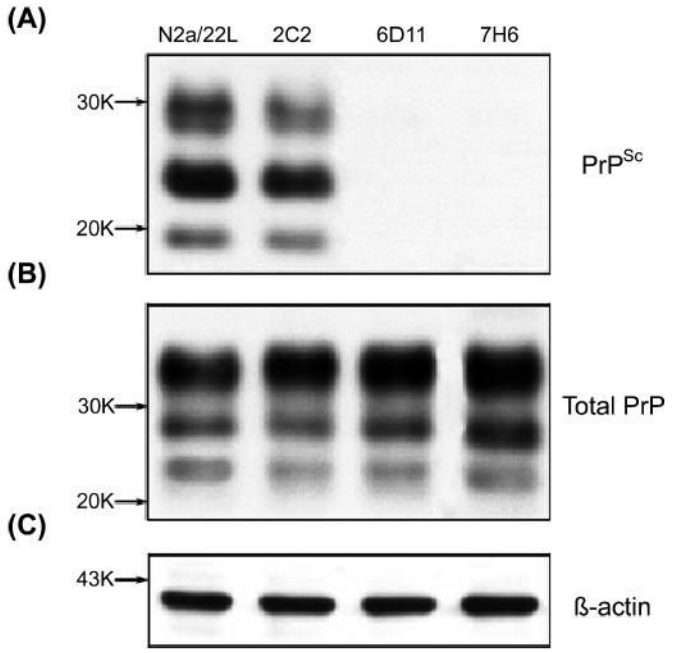

Fig. 6.
Protein expression in N2a/22L cells treated with Mabs 2C2, 6D11 and 7H6. (A) Level of PrP^{Sc} following PK digestion; (B) level of total PrP; (C) level of β-actin.

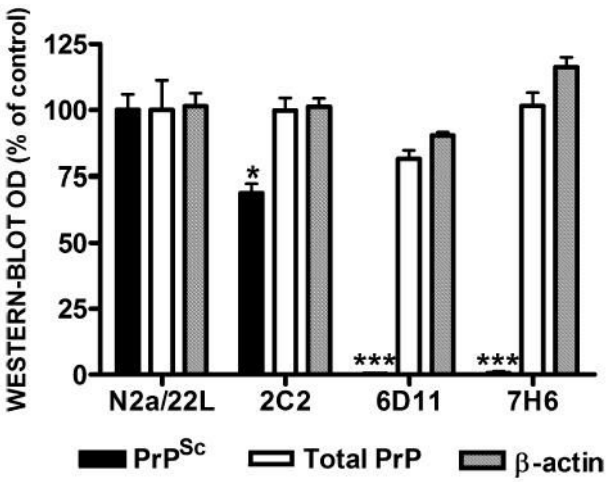

Fig. 7.

Quantification of protein expression in N2a/22L cells treated with Mabs. While 2C2 resulted in partial reduction in PrP^{Sc} and 6D11 and 7H6 caused complete abrogation of PrP^{Sc}, treatment with these Mabs did not significantly affect either the total level of PrP (PrP^{C} + PrP^{Sc}) or the level of unrelated proteins such as β-actin. Values are given as mean + SD from at least three independent experiments. One-way ANOVA ($P < 0.0001$) was followed by Dunnett's *post hoc* test; *$P < 0.05$, ***$P < 0.001$.

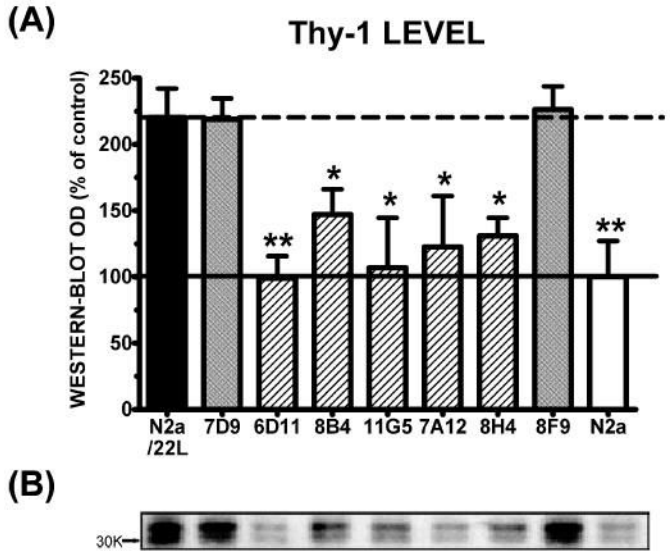

Fig. 8.

(A) The level of Thy-1 in N2a/22L cells treated with various Mabs. The level of Thy-1 in N2a/22L cells was more than twice than in N2a cells. Mabs 7D9 and 8F9, which showed no significant therapeutic effect, had no impact on the Thy-1 level. Incubation of N2a/22L cells with therapeutically effective Mabs caused a significant reduction in Thy-1 level. One-way ANOVA ($P < 0.001$) was followed by a Dunnett *post hoc* test; *$P < 0.05$, **$P < 0.01$. (B) Thy-1 in cell lysates following treatment with specific Mabs.

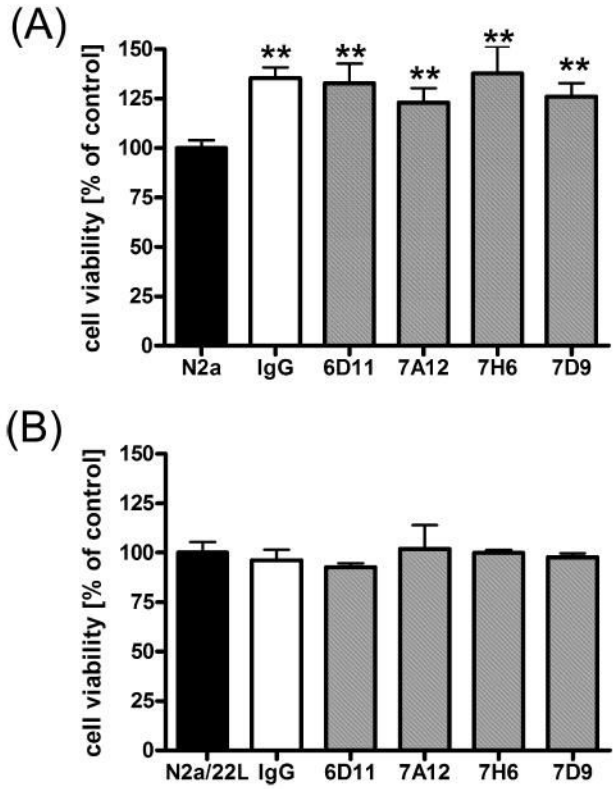

Fig. 9.

The effect of Mabs on viability of N2a and N2a/22L cells. (A) Murine IgG and anti-PrP Mabs had a nonspecific trophic effect on N2a cells. One-way ANOVA ($P < 0.0001$) was followed by Dunnett's *post hoc* test; **P < 0.01. (B) Anti-PrP Mabs showed neither a trophic effect nor reduced viability of N2a/22L cells. Values are given as a mean + SD from six independent measurements.

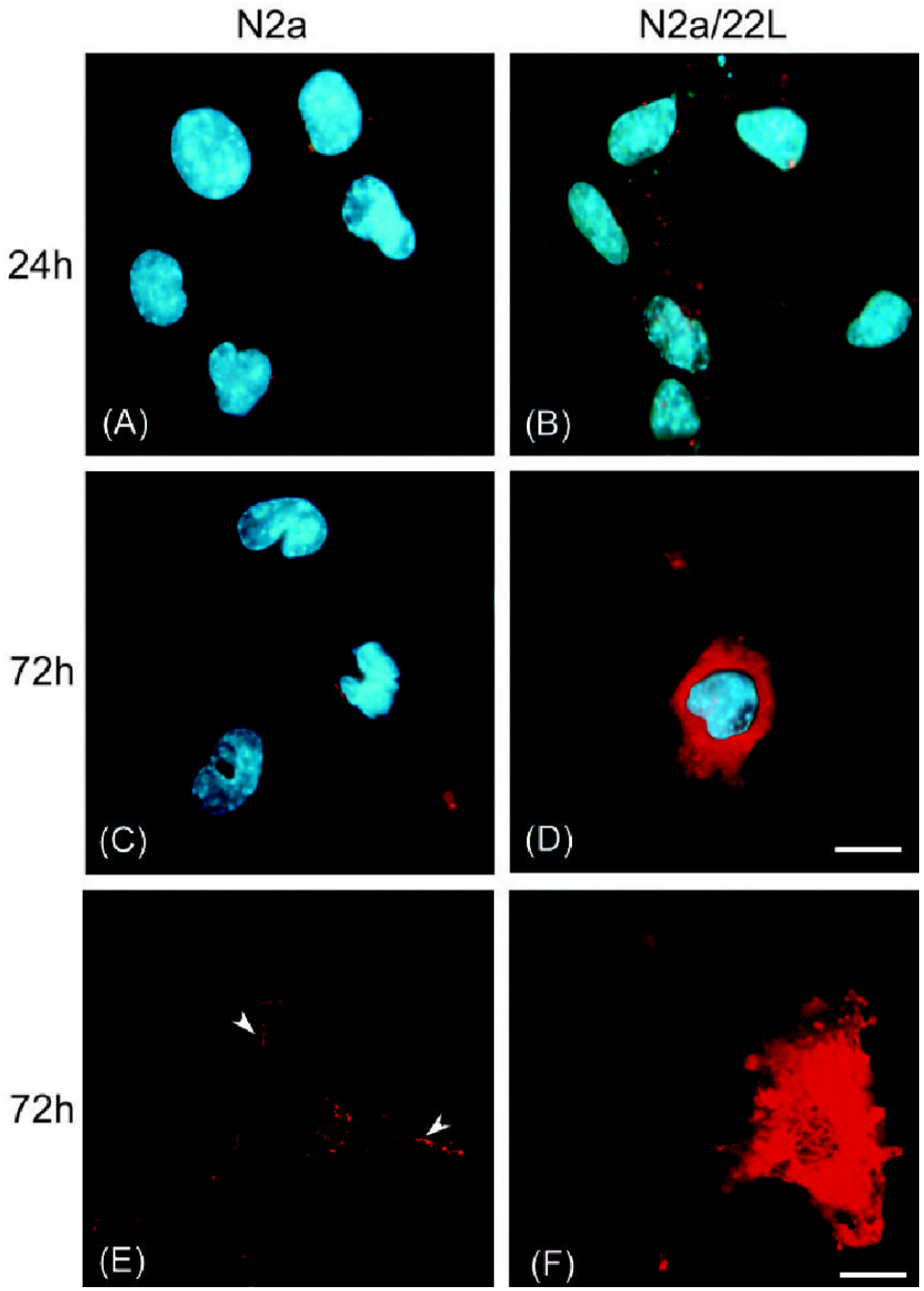

Fig. 10.

Incubation of N2a and N2a/22L cells in the presence of Mab 6D11 conjugated with Cy3 (6D11/Cy3). Labeling of the plasma membrane in N2a cells grown in the presence of 6D11/Cy3 for (A) 24 h and (C) 72 h. (E) Confocal microscopy images showing binding of Mabs to the outer leaflet of the plasma membrane (arrowheads). (B) In addition to membrane labeling, N2a/22L cells showed internalization of 6D11/Cy3 after 24 h, which (D and F) was more pronounced after 72 h. A–D, deconvolution microscope; E and F, confocal microscope. Red staining in A–F represents Cy3; blue staining in A–D is DAPI nuclear dye. Scale bars, 10 μm (in D for A–D), 20 μm (in F for E and F).

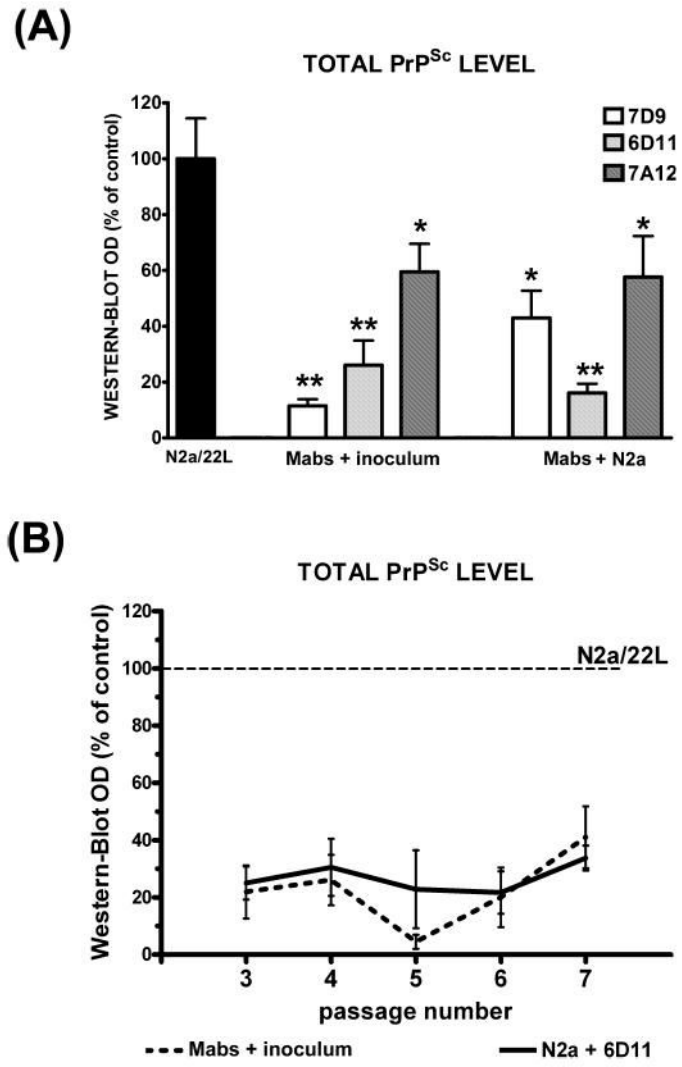

Fig. 11.

(A) Decreased level of PrP^{Sc} in the third passage of N2a/22L cells which were infected with inoculum preincubated with Mabs (Mabs + inoculum) or N2a cells incubated with Mabs before being exposed to the inoculum (Mabs + N2a); results are compared to the level of PrP^{Sc} in N2a/22L cells infected in a standard manner. Values are given as mean + SD from at least three independent experiments. One-way ANOVA ($P < 0.0001$) was followed by Dunnett's *post hoc* test; $*P < 0.05$, $**P < 0.01$. (B) Persistently decreased level of PrP^{Sc} was maintained in subsequent passages of N2a cells infected in the presence of 6D11. Values are given as mean ± SD from at least three independent experiments. Comparison was made to the density of PrP^{Sc} bands (designated as 100%) in corresponding passages of N2a/22L cells infected in the standard manner (repeated-measures ANOVA; $P < 0.001$).

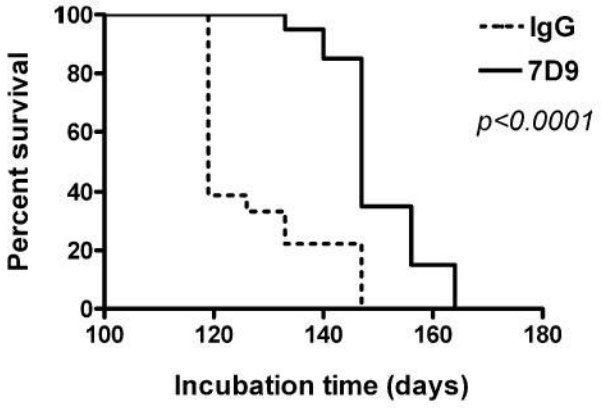

Fig. 12.

Kaplan–Meier survival analysis of CD-1 mice prophylactically treated with a single dose of Mab 7D9 administered immediately after intraperitoneal exposure to 22L brain homogenate. Animals which received Mab 7D9 showed a statically significant delay in onset of neurological symptoms compared to those which received an equivalent dose of IgG. Log rank test indicates a statistically significant difference between the groups ($P < 0.0001$).

Table 1

Characterization of anti-PrP Mabs

Antibody	Antigen localization†	K_D
7D9	Unknown, nonlinear	$8.2 \pm 0.19 \times 10^{-10}$M
8B4	35–45	$2.4 \pm 0.60 \times 10^{-10}$M
6D11	93–109	$8.5 \pm 0.18 \times 10^{-11}$M
11G5	115–130 (1st β-strand)	$5.4 \pm 0.17 \times 10^{-10}$M
7H6	130–140	$2.2 \pm 0.04 \times 10^{-10}$M
7A12	143–155 (α-helix A)	$1.9 \pm 0.05 \times 10^{-10}$M
2C2	153–165 (2nd β-strand)	$3.4 \pm 0.15 \times 10^{-9}$M
8H4	175–185 (α-helix B)	$3.8 \pm 0.11 \times 10^{-10}$M
9H7	143–231	$10.3 \pm 0.43 \times 10^{-10}$M
8F9	220–231	$10.6 \pm 0.50 \times 10^{-9}$M

† Numbers correspond to residues of murine PrP. K_D values are given as mean ± SD from at least three independent experiments.